

## Two-Nucleon Photon Absorption on ${}^3\text{He}$ in the $\Delta(1232)$ Region

N. d'Hose, G. Audit, A. Bloch, N. de Botton, L. Jammes, J. M. Laget, J. Martin, E. Mazzucato,  
A. Sasaki, C. Schuhl, and G. Tamas

*Service de Physique Nucléaire-Haute Energie, Centre d'Etudes Nucléaires de Saclay,  
91191 Gif-sur-Yvette CEDEX, France*

L. Ghedira, M. Rodgers, and P. Stoler

*Physics Department, Rensselaer Polytechnic Institute, Troy, New York 12181*

P. Argan and P. Pedroni

*Instituto Nazionale di Fisica Nucleare, Sezione di Pavia, Via Bassi 6, Pavia, Italy*

(Received 3 October 1988)

Cross sections were determined in the  $\Delta(1232)$  excitation region for the reactions  ${}^3\text{He}(\gamma,p)pn$  and  ${}^2\text{H}(\gamma,p)n$  at several photon energies and proton emission angles. Inclusive proton spectra were measured with a magnetic spectrometer, using a quasimonochromatic  $e^+$ -annihilation photons. The  ${}^3\text{He}$  data can be mainly accounted for by predictions assuming photon absorption by a pair of nucleons, except in the high-momentum part of the proton spectra. They clearly indicate the need for additional contributions, such as three-body absorption mechanisms.

PACS numbers: 25.20.Dc, 25.10.+s

This paper deals with the process in which an incident photon is absorbed on a nucleus and no pions are present in the final state. Because of the large mismatch between photon and nucleon momenta, photon absorption on a single nucleon is strongly inhibited. The photon is thus predominantly absorbed by few-nucleon subsystems, allowing the energy and momentum to be shared by several nucleons. Absorption by a correlated neutron-proton pair is thought to be the dominant reaction mechanism; it has led to the phenomenological quasideuteron model of Levinger.<sup>1</sup> Recent measurements suggest that, in the  $\Delta$  region, the analogous process of pion true absorption involves, in addition to the two-body mode, a significant contribution of a three-body mode.<sup>2,3</sup>

Measurements of inclusive proton photoproduction spectra on light nuclei<sup>4,5</sup> have shown the presence of a prominent peak corresponding to the kinematics of the quasifree two-nucleon photon absorption. However, it is on a simple system such as  ${}^3\text{He}$  that a detailed comparison with theory is possible. Indeed, in this case "exact" wave functions are available and the final-state interaction (FSI) can be treated at an elementary level. Furthermore, the simultaneous measurement of  ${}^3\text{He}(\gamma,p){}^2\text{H}$  and  ${}^2\text{H}(\gamma,p)n$  cross sections allows one to control the different ingredients of the calculation. This paper reports precisely the first measurement of the  ${}^3\text{He}(\gamma,p)$  reaction for several photon energies (208, 248, 278, 308, and 338 MeV) and proton emission angles ( $23^\circ$ ,  $46^\circ$ , and  $58^\circ$ ).

The present experiment was carried out at the Saclay linac with quasimonochromatic photons from in-flight positron annihilation. This facility and the experimental technique are described elsewhere.<sup>6</sup> A positron beam, with maximum available energy  $E^+ = 550$  MeV and current of 50 nA, impinges on a liquid-hydrogen radiator

of thickness 9.6 cm. The annihilation photons are collimated in the forward direction, resulting in a beam of energy very nearly  $E^+$ , 1% resolution, and flux about  $5 \times 10^7/\text{s}$ . A bremsstrahlung beam is also produced. The resulting proton spectrum is due to both of these components of the photon beam. The bremsstrahlung proton spectrum is subtracted by repeating the measurement under the same kinematical conditions, using a copper radiator of the same thickness in radiation lengths as the hydrogen radiator. The former produces a nearly pure bremsstrahlung spectrum because of its high  $Z$ . A small correction is made which takes into account the difference in shape between the hydrogen and copper bremsstrahlung spectra. The photon flux was monitored using a Wilson gas quantameter whose calibration constant is determined with an accuracy better than 1%.

Proton momentum spectra were obtained with the "700" magnetic spectrometer (2.2 msr, momentum acceptance 12% divided in 16 bins), whose focal plane is instrumented with an array of plastic scintillator detectors, which are used for momentum analysis and particle identification.

The reaction target consisted of liquid  ${}^3\text{He}$  in a thin-walled cylindrical container of diameter 7 cm and height 4.5 cm. The beam diameter defined by the collimators was 3 cm. Two other identical vessels contained liquid  ${}^2\text{H}$  and  ${}^1\text{H}$ . The latter was used to determine the small background contribution.

The system response shape obtained with a Monte Carlo simulation, which includes the geometry of the experimental setup and the kinematics broadening, was convoluted with the photon spectrum yielding the overall experimental response function. This was found to agree well with that observed by measuring the  ${}^2\text{H}(\gamma,p)n$  reaction as shown in Fig. 1. As discussed below, the  ${}^2\text{H}$  data

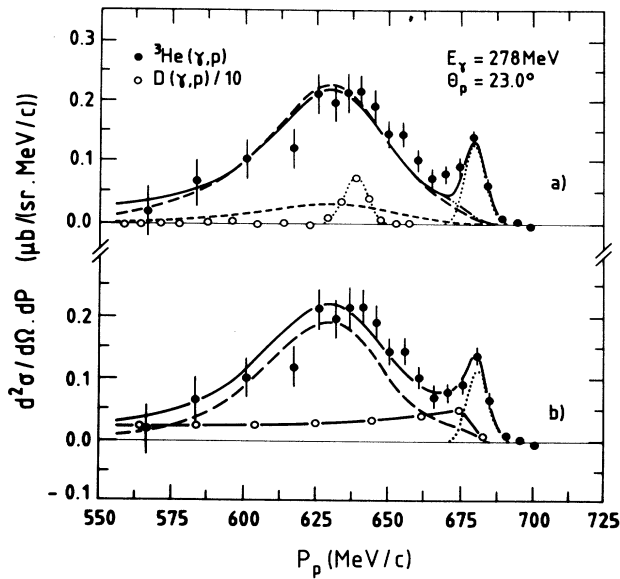


FIG. 1. (a) Cross section measured at  $\theta_p = 23^\circ$  and  $E_\gamma = 278$  MeV for  ${}^3\text{He}(\gamma, p)$  (filled circles) and  ${}^2\text{H}(\gamma, p)n$  (open circles). The latter is divided by 10 and compared with the overall experimental response function. Also shown is the theoretical result (Refs. 7 and 8) without any renormalization. Dotted curve: the  ${}^3\text{He}(\gamma, p)d$  reaction; short-dashed curve: photodisintegration of a correlated pair [diagrams in Fig. 2(a)]; long-dashed curve: two-nucleon photodisintegration including pion exchange and FSI [diagrams of Figs. 2(a) and 2(b)]; dash-dotted curve: the same as above with the three-nucleon absorption [diagrams of Fig. 2(c)]; solid curve: sum of dotted and dash-dotted curves. (b) The result of the empirical fit to the data. Dotted curve: the  ${}^3\text{He}(\gamma, p)d$  reaction; dashed curve: two-nucleon absorption with FSI; dash-dotted curve: three-nucleon absorption with FSI; solid curve: sum of the three components.

are compared with the  ${}^3\text{He}$  data measured at the same kinematical conditions, thereby minimizing systematic errors in the  ${}^3\text{He}/{}^2\text{H}$  ratio.

Figure 1 also shows the proton momentum spectrum from  ${}^3\text{He}$  due to 278-MeV annihilation photons. Two features are apparent. The small peak at the high-momentum limit corresponds to the channel  ${}^3\text{He}(\gamma, p){}^2\text{H}$ . The large broad peak with a maximum near  $P_p = 640 \text{ MeV}/c$  is the contribution corresponding to the  ${}^3\text{He}(\gamma, p)np$  channel. This is a clear signature of the absorption of the interacting photon by a quasifree nuclear pair: Its maximum occurs at the momentum of a proton emitted at the same angle as in the reaction  ${}^2\text{H}(\gamma, p)n$ , and its width is nearly constant as a function of photon energy at a given angle. The shape is well reproduced by a quasifree calculation which employs the experimental momentum distribution<sup>9</sup> of the pair. These features are also reproduced by a multiple-scattering calculation<sup>7</sup> which was carried out within a Lagrangian framework, considering diagrams shown in Fig. 2. The  ${}^3\text{He}$  wave function is the solution to Faddeev equations using a

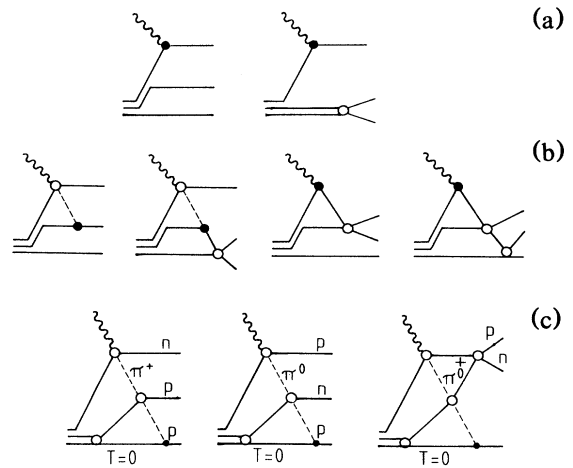


FIG. 2. Diagrams of photodisintegration. (a) Correlated pair; (b) pion exchange and FSI; (c) three-nucleon absorption.

Reid nucleon-nucleon interaction. The continuum wave function is taken as the sum of a plane wave and half-off-shell nucleon-nucleon scattering amplitudes for the same potential. The results of the calculation are shown in Fig. 1(a). The short-dashed curve is due to absorption on a correlated nucleon pair, as in the diagrams of Fig. 2(a). The long-dashed curve is obtained by adding the diagrams of Fig. 2(b) which include the two-nucleon meson exchange. Clearly, the two-nucleon process accounts for most of the cross section, except at the highest momenta, where the calculated effect of the FSI cannot reproduce the data. The dash-dotted curve also includes the three-body contribution<sup>8</sup> [diagrams of Fig. 2(c)] corrected for FSI, which is part of the three-nucleon absorption process. This mechanism results in a small increase near the proton maximum momentum, but dominates below the quasideuteron peak, outside the range of momentum covered by the present experiment, enhancing the total calculated integrated photodisintegration cross section by a factor of 2. The dotted curve at the high-momentum end of the spectrum accounts for the  ${}^3\text{He}(\gamma, p){}^2\text{H}$  reaction.<sup>10</sup>

The solid curve, which includes all the contributions, describes the data well, except between the quasifree and the  ${}^3\text{He}(\gamma, p){}^2\text{H}$  peaks, where the model still underestimates the cross section. This effect persists at all photon energies and proton angles. Tentatively we attribute this discrepancy to three-nucleon absorption mechanisms.

In order to extract the two-nucleon part of the cross section, and obtain a quantitative indication of the size of the three-nucleon contribution, we follow the method used in Refs. 2 and 3 to analyze the pion-true-absorption reactions, where it was found that the three-nucleon absorption is large, and consistent with a phase-space distribution.

In this method each proton spectrum is taken to be the

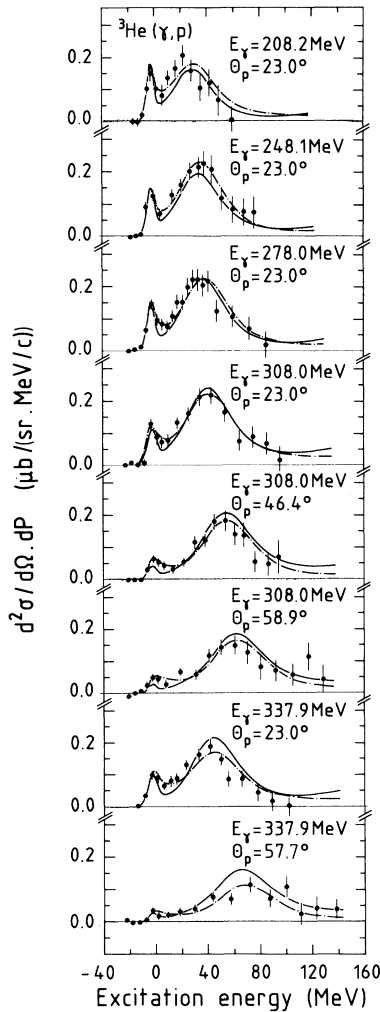


FIG. 3. The differential cross section as a function of the excitation energy for various photon energies and various angles. Solid curve: the theoretical model prediction; dash-dotted curve: the empirical fit.

incoherent sum of the following three contributions: (i) the  ${}^3\text{He}(\gamma,p){}^2\text{H}$  line which is not completely resolved because of the momentum resolution; (ii) the absorption of the photon by a nucleon pair with a Fermi motion described by the experimental momentum distribution measured in the  ${}^3\text{He}(e,e'p)X$  experiment,<sup>9</sup> corrected for the FSI of the two undetected nucleons following the same procedure as in Ref. 7; (iii) the three-nucleon photoabsorption assumed to follow a simple three-body phase space, corrected for the FSI according to the Watson formula.<sup>11</sup>

These contributions were folded with the experimental response and their amplitudes varied to obtain the minimum  $\chi^2$ . Considering only the first two components, we obtained  $\chi^2=261$  for 110 degrees of freedom. When the three-body contribution was included, a significant improvement was obtained:  $\chi^2=117$  for 102 degrees of freedom. The corresponding fit, and the individual contributions, are presented in Fig. 1(b).

Figure 3 shows the measured differential cross sections as a function of the excitation energy of the undetected two-nucleon system. The solid curves are the theoretical model prediction and the dash-dotted curves are the results of the empirical fit described above. All the data confirm the dominance of the two-nucleon absorption process in the momentum range covered by the experiment, and require additional contributions at the high-momentum part of the distribution, which may be indicative of three-nucleon photon absorption.

In Table I we present the following: (i) The momentum integrated experimental cross sections for the  ${}^3\text{He}(\gamma,p)pn$  channel, and the differential cross sections for the  ${}^2\text{H}(\gamma,p)n$  reaction. (ii) The two-nucleon-absorption cross section, extracted from the empirical fit. It is compared to the  ${}^2\text{H}$  photodisintegration cross section, yielding a ratio of  $1.68 \pm 0.07$ , relatively independent of the kinematical conditions; this is in reasonable agreement with the theoretical model prediction of 1.79 (in a

TABLE I. (a) Experimental differential cross section  $d\sigma/d\Omega$  integrated over the momentum range of the data. This momentum range was defined to cover 95% of the two-body differential cross section determined from the theoretical model. (c) The ratio of the  ${}^3\text{He}$  two-body differential cross section, deduced from the empirical fitting procedure, to the corresponding measured  ${}^2\text{H}$  cross section. This is compared to the theoretical result given in column (b). (d) The total three-body cross section deduced from the empirical fitting procedure assuming a three-body phase-space dependence.

$E_\gamma$ (MeV)	$\theta_{\text{lab}}$ (deg)	Experiment $d\sigma/d\Omega$ ( $\mu\text{b}/\text{sr}$ )		Theoretical model	Empirical fit	
		${}^2\text{H}$	${}^3\text{He}$ (a)	$2N-{}^2\text{H}$ (b)	$2N-{}^2\text{H}$ (c)	$\sigma(3N)$ ( $\mu\text{b}$ ) (d)
208.2	23.0	$6.35 \pm 0.26$	$12.64 \pm 1.93$	1.94	$1.33 \pm 0.25$	$75.5 \pm 20.5$
248.1	23.0	$6.77 \pm 0.24$	$14.11 \pm 1.55$	1.76	$1.80 \pm 0.19$	$48.5 \pm 18.2$
278.0	23.0	$7.18 \pm 0.36$	$14.49 \pm 1.19$	1.71	$1.59 \pm 0.16$	$69.0 \pm 13.7$
308.0	23.0	$6.50 \pm 0.36$	$14.63 \pm 1.45$	1.76	$1.71 \pm 0.20$	$78.2 \pm 18.3$
308.0	46.4	$5.98 \pm 0.28$	$12.81 \pm 1.14$	1.74	$1.81 \pm 0.19$	$49.8 \pm 12.4$
308.0	58.9	$5.33 \pm 0.21$	$12.84 \pm 1.35$	1.77	$1.87 \pm 0.24$	$66.1 \pm 13.5$
337.9	23.0	$5.24 \pm 0.23$	$11.77 \pm 1.08$	1.82	$1.53 \pm 0.17$	$81.0 \pm 14.2$
337.9	57.7	$3.66 \pm 0.16$	$8.57 \pm 1.21$	1.83	$1.92 \pm 0.30$	$43.7 \pm 12.9$

naive model involving only  $s$ -wave nucleons, there are 1.5 isoscalar neutron-proton pairs in  ${}^3\text{He}$ ). (iii) The three-body cross section obtained in the fit. It shows no strong energy dependence and is about 60% of the two-body one taken to be  $1.68 \pm 0.07$  times the experimental deuterium total cross section;<sup>12</sup> this figure should be compared with the pion-absorption one which ranges from 25% to 60%.<sup>2,3</sup>

In summary, we have clearly observed the two-nucleon absorptive mechanism in  ${}^3\text{He}$  in the  $\Delta$  excitation region. Its size agrees with the predictions of a microscopic model based on realistic wave functions. We tentatively interpret the cross-section excess at the high-energy side of the two-nucleon-absorption distribution as due to a three-body contribution with a phase-space distribution. This cross-section excess is much larger than that predicted by a multiple-scattering calculation involving sequential meson-nucleon scattering processes; we consider this as a suggestion for an additional three-body contribution.

Three-body contributions are expected to dominate the low-momentum part of the proton spectrum, which cannot be observed using the present experimental method because of the large component of bremsstrahlung con-

taminating the positron-annihilation beam. The study of the  ${}^3\text{He}(\gamma, p)pn$  and of the more exclusive  ${}^3\text{He}(\gamma, NN)N$  reactions outside the quasideuteron region, using a tagged photon beam and large-acceptance detectors at the new continuous-wave facilities, would be particularly welcome to better pin down the three-body mechanism.

P.S. acknowledges partial support from the NSF Grant No. PHY.8601006.

---

<sup>1</sup>J. L. Levinger, Phys. Rev. **84**, 43 (1951).

<sup>2</sup>G. Backenstoss *et al.*, Phys. Rev. Lett. **55**, 2782 (1985); **59**, 767 (1987).

<sup>3</sup>K. A. Aniol *et al.*, Phys. Rev. C **33**, 1714 (1986).

<sup>4</sup>S. Homma *et al.*, Phys. Rev. Lett. **45**, 706 (1980); Phys. Rev. C **36**, 1623 (1987).

<sup>5</sup>J. Arends *et al.*, Z. Phys. A **298**, 103 (1980).

<sup>6</sup>J. L. Faure *et al.*, Nucl. Phys. **A424**, 383 (1984).

<sup>7</sup>J. M. Laget, Phys. Lett. **151B**, 325 (1985).

<sup>8</sup>J. M. Laget, J. Phys. G **14**, 1445 (1988).

<sup>9</sup>E. Jans *et al.*, Phys. Rev. Lett. **49**, 974 (1982).

<sup>10</sup>J. M. Laget, Phys. Rev. C **38**, 2993 (1988).

<sup>11</sup>M. L. Goldberger and K. M. Watson, *Collision Theory* (Wiley, New York, 1964).

<sup>12</sup>J. Arends *et al.*, Nucl. Phys. **A412**, 509 (1984).